J. Synchrotron Rad. (1999). **6**, 549–551

Local structure in crystalline and liquid tellurium probed by X-ray absorption spectroscopy

Simone De Panfilis,[a]* Adriano Filipponi[a,b] and Carlo Meneghini[c,d]

[a]European Synchrotron Radiation Facility, B.P. 220, F-38043 Grenoble, France, [b]Dip. di Fisica, Università dell'Aquila, I-67010 L'Aquila, Italy, [c]INFN - Laboratori Nazionali di Frascati, Via E. Fermi 40, I-00044 Frascati, Italy, and [d]INFM - GILDA c/o ESRF, B.P. 220, F-38043 Grenoble, France. E-mail: panphili@esrf.fr

We have performed high-quality X-ray absorption measurements on crystalline (*c*-Te) and liquid (ℓ-Te) tellurium. Performing a consistent analysis that takes into account the contribution of the medium range structure, we have determined reliable pair correlation functions in ℓ-Te up to 3.5 Å, and we confirm the existence of stronger and weaker first-neighbour interactions, responsible of the band-gap filling at the Fermi level. A complete *ab initio* multiple scattering calculation have been applied to evaluate temperature dependence of short-range properties in *c*-Te.

Keywords: liquid metals; structure of liquids; X-ray absorption spectroscopy.

1. Introduction

Since the early studies on liquid tellurium (ℓ-Te) (Cabane & Friedel, 1971, Waseda *et al.*, 1975), the correlation between structural and electronic transition as a function of temperature remained an interesting and challenging problem in the field of liquid metals (Enderby & Barnes, 1990). Similarly to the other chalcogens like sulfur or selenium, crystalline tellurium (*c*-Te) is a twofold coordinated semiconductor (Adenis *et al.*, 1989); but, unlike Se, it loses its semiconducting behaviour upon melting and it becomes a (semi-)metal.

Pursuing this long-standing question, a large number of different experimental structural probes (Waseda *et al.*, 1975, Thurn & Ruska, 1976, Mennelle *et al.*, 1987, Tamura *et al.*, 1991, Tsuzuki *et al.*, 1995, De Panfilis & Filipponi, 1997) have been applied, and some theoretical insight have been recently achieved (Hafner, 1990, Bichara *et al.*, 1996).

As a consequence of this intensive study, it is now believed that the twofold chain structure characteristic of the trigonal crystalline tellurium still survives in ℓ-Te. The coexistence of covalent bonds and metallic character in the liquid phase, thus, results into an anomalous behaviour of the electrical conductivity as a function of temperature (Cabane & Friedel, 1971). It has been shown that a major role in the description on the metallisation in ℓ-Te is played by the mutual distance of the chains (inter-chain bond).

In the present paper, thus, we report an X-Ray absorption spectroscopy (XAS) study of crystalline and liquid tellurium as a function of temperature. We present a full analysis up to the 10th coordination shell in *c*-Te, and a detailed description of the atomic arrangement in ℓ-Te, which complement a previous study already published (De Panfilis & Filipponi, 1997).

2. Experimental and data analysis

XAS measurements have been performed at the EXAFS beamline (BM29) of the European Synchrotron Radiation Facility (ESRF). The details of the synchrotron working conditions and of the X-ray beam have been described elsewhere (De Panfilis *et al.*, 1998).

Samples were prepared following a well established technique (Filipponi & Di Cicco, 1994). A fine powder of TeO_2 was ball-milled together with ultra-pure graphite powder in 1:20 dilution in order to achieve the requested sample homogeneity and then pressed into pellets. *In situ* reduction in high vacuum to the pure elements was monitored by means of successive rapid near edge scans. A single energy X-ray absorption detection (SEXAD) (Filipponi *et al.*, 1998) as a function of temperature performed on a reduced sample is presented in Fig. 1: the occurrence of a sharp melting transition is characteristic of a high-purity bulk sample. Eventually, the presence of a single *c*-Te phase in the measured samples was checked performing powder X-ray diffraction (XRD).

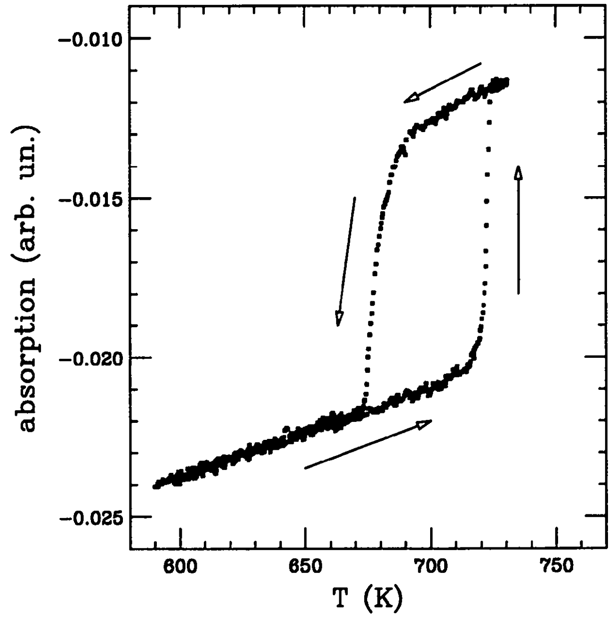

Figure 1
SEXAD pattern at E= 31.8829 keV as a function of temperature for high-purity Te. The hysteresis cycle shows a sharp melting transition at T_m = 722.6 K on the heating stroke and an undercooled metastable state of about 50°C during the cooling period.

The crystalline samples have been measured at various temperature, from 20 K up to the melting point T_m. Spectra of ℓ-Te have been collected in the liquid and in the undercooled state.

XAS signals $\chi(k)$ have been analysed within the GNXAS data analysis framework (Filipponi *et al.*, 1995), including 2-body and, where appropriate and sensible, 3-body terms. In Tab. 1 are presented the determined values for the intra- and inter-chain structural parameters, at different temperature, for *c*-Te; the coordination numbers, 2 and 4 respectively, have been kept fixed. Anharmonic effects in high temperature spectra of *c*-Te have been taken into account by means of asymmetric coordination shells. An example of the best fit procedure result is also shown in Fig. 2 for the 20 K case.

Table 1

Intra-chain (R_1, σ_1^2) and inter-chain (R_2, σ_2^2) structural parameters for *c*-Te as determined from the present study, as a function of temperature. The statistical errors are calculated taking into account correlations with other relevant fitting parameters.

T (K)	R_1 (Å)	σ_1^2 (Å^2)
20	2.8361±.0027	$(1.63\pm.21)10^{-3}$
40	2.8365±.0023	$(1.67\pm.19)10^{-3}$
100	2.8341±.0033	$(2.14\pm.16)10^{-3}$
170	2.8321±.0052	$(3.49\pm.35)10^{-3}$
200	2.8319±.0053	$(3.75\pm.35)10^{-3}$
300	2.8299±.0063	$(5.44\pm.32)10^{-3}$
T (K)	R_2 (Å)	σ_2^2 (Å^2)
20	3.4792±.0043	$(3.23\pm.31)10^{-3}$
40	3.4847±.0045	$(3.77\pm.29)10^{-3}$
100	3.4830±.0059	$(6.38\pm.45)10^{-3}$
170	3.4906±.0074	$(11.1\pm1.6)10^{-3}$
200	3.507±.011	$(12.7\pm1.7)10^{-3}$
300	3.545±.013	$(23.1\pm1.8)10^{-3}$

Liquid tellurium measurements have been treated following a consistent data analysis method (Crozier *et al.*, 1988, A. Filipponi, 1994, De Panfilis & Filipponi, 1997) that takes into account long-range asymptotic behaviour contained in the $S(q)$ previously measured by neutron diffraction (ND) (Mennelle *et al.*, 1987). The resulting best fit for the 800 K spectra is presented in Fig. 3. The determined pair correlation function $g(R)$ has been found to be in nice agreement with the ND model and with previous XAS (Tamura *et al.*, 1991, Tsuzuki *et al.*, 1995) determinations, based on a standard two-shell fittin procedure.

3. Results and discussion

It is known that Te undergoes a peculiar anisotropical thermal expansion, actually presenting a contraction along the *c* unit cell direction. The interaction of primary (intra-chain, R_1) and secondary (inter-chain, R_2) bonding (Martin *et al.*, 1976) in *c*-Te shows that secondary bonds develop covalent character and weaken primary bonds: in principle, when $R_1=R_2$, the two types of bonds are indistinguishable and the solid is a metal. This is very well shown in Tab. 1 where the contraction of the distance between the chain on lowering the temperature results in an increasing value for R_1, i.e., there is a weakening of primary bonding and a strengthening of secondary one.

Nevertheless, the mixing of the two bonding is never big enough to allow tellurium to become a metal at any low temperature.

Instead, the substantial penetration of at least an atom well below the distance of the nearest inter-chain bonds occurs in ℓ-Te. This comes out evident if one looks at the comparison of the average structure in solid and liquid Te, which is reported in Fig. 4, both for the $g(R)$ and for the running coordination number $N(R)$. The gap between 3 and 3.3 Å separating the first two peaks in the pair correlation function is filled by novel distances, and, regarding to the $N(R)$ curve, this corresponds quantitatively to one atom penetration.

Thus, a significant overlap of the charge density in the antibonding lone-pair orbitals (Joannopoulos *et al.*, 1975) occurs, and the electronic band gap at the Fermi level is filled.

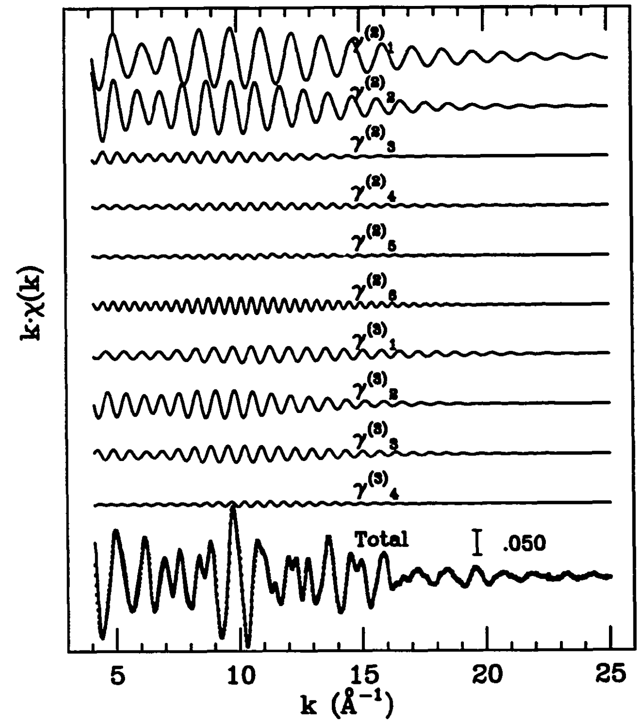

Figure 2

Best fit (continuous line) of experimental data (points): at 20 K. The signals associated with the relevant 2-body ($\gamma^{(2)}$) and 3-body ($\gamma^{(3)}$) paths are also shown.

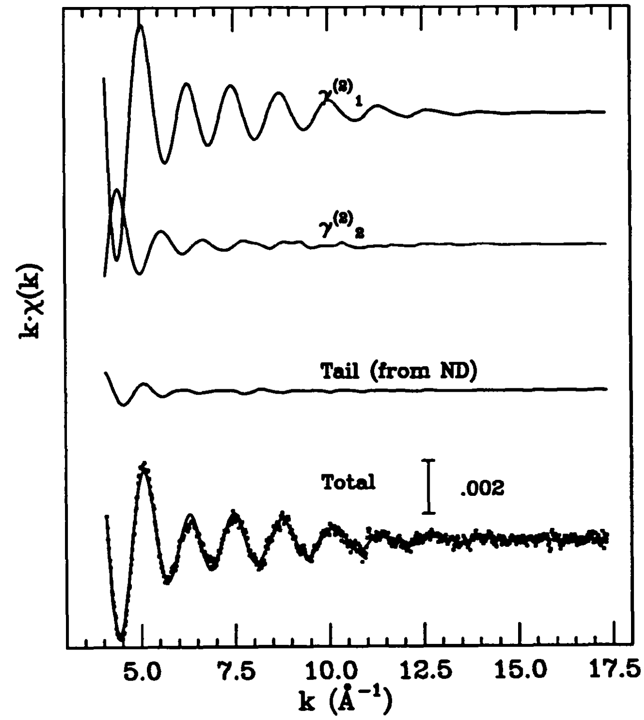

Figure 3

Best fit (continuous line) of experimental data (points): at 800 K (b). The signals associated with the two Γ-like ($\gamma^{(2)}$) distributions and the tail are also presented.

The present study shows the potential of a careful XAS investigation on a mono–atomic system. Reliable $g(R)$ for solid and liquid Te have been determined and evidence for the coexistence of stronger and weaker first neighbour interactions was presented to explain the semiconductor–to–(semi-)metal transition observed in Te upon melting.

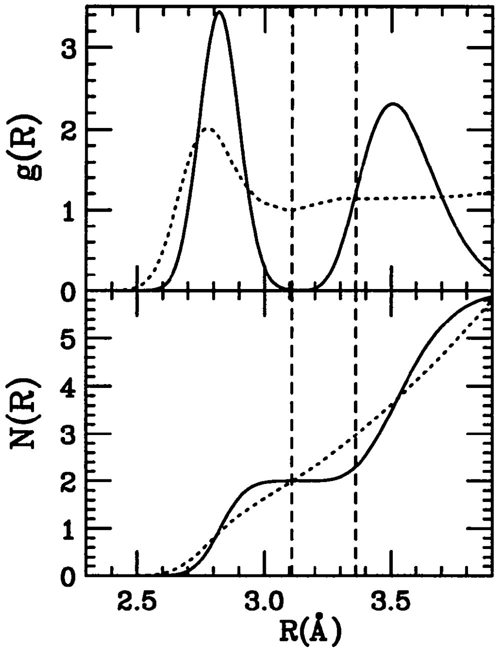

Figure 4

Comparison between the present XAS structural determination of g(R) (upper panel) and the running coordination number N(R) (lower panel) in *c*-Te at 297 K (solid line) and *ℓ*-Te at 800 K (dots).

Experiments have been performed at the ESRF (beamlines BM29 and BM16) during beamtime allocated for the proposals HE-156, SC-360 and HE-259. We acknowledge F. Sperandini and M. Minicucci for continuous support during data acquisition. The helpful assistance of Dr. A. Balerna in performing and discussing XRD measurements has been highly appreciated.

References

C. Adenis, V. Langer & O. Lindqvist (1989). *Acta Cryst. C* **45**, 941–942.

C. Bichara, J.-Y. Raty & J.-P. Gaspard (1996). *Phys. Rev. B* **53**, 206–211.

B. Cabane & J. Friedel (1971). *J. Physique* **32**, 73–84.

E. D. Crozier, J. J. Rehr & R. Ingalls (1988), in *X-ray Absorption*, edited by D. C. Konigsberger & R. Prins, pp. 373–442, New York: J. Wiley & Sons.

S. De Panfilis & A. Filipponi (1997). *Europhys. Lett.* **37**, 397–402.

S. De Panfilis, A. Filipponi & C. Meneghini (1998). *Electronic archive for experimental and data analysis details*, XAFS X Conference.

J. E. Enderby & A. C. Barnes (1990). *Rep. Prog. Phys.* **53**, 85–118.

A. Filipponi & A. Di Cicco (1994). *Nucl. Inst. & Methods for Phys. Res. B* **93**, 302–307.

A. Filipponi (1994). *J. Phys.: Condens. Matter* **6**, 8415–8427.

A. Filipponi, A. Di Cicco, & C. R. Natoli (1995). *Phys. Rev. B* **52**, 15122–15134; **52**, 15135–15145.

A. Filipponi, M. Borowski, P. W. Loeffen, S. De Panfilis, A. Di Cicco, F. Sperandini, M. Minicucci & M. Giorgetti (1998). *J. Phys.: Condens. Matter* **10**, 235–253.

J. Hafner (1990) *J. Phys.: Condens. Matter* **2**, 1271–1280.

J. D. Joannopoulos, M. Schlüter & M. L. Cohen (1975). *Phys. Rev. B* **11**, 2186–2199.

R. M. Martin, G. Lucovsky & K. Helliwell (1976). *Phys. Rev. B* **13**, 1383–1395.

A. Mennelle, R. Bellissent & A. M. Flank (1987). *Europhys. Lett.* **4**, 705–708.

K. Tamura, M. Inui, M. Yao, H. Endo, S. Hosokawa, H. Hoshino, Y. Katayama & K. Maruyama (1991). *J. Phys.: Condens. Matter* **3**, 7495–7510.

H. Thurn & J. Ruska (1976). *J. Non-Cryst. Solids* **22**, 331–343.

T. Tsuzuki, M. Yao & H. Endo (1995). *J. Phys. Soc. Jpn.* **64**, 485–503.

Y. Waseda & S. Tamaki (1975). *Z. Naturforsch.* **30**, 1655–1660.

(*Received 10 August 1998; accepted 11 December 1998*)